PHYSICAL REVIEW E VOLUME 47, NUMBER 1 JANUARY 1993

Activated dynamics, loss of ergodicity, and transport in supercooled liquids

D. Thirumalai
Institute for Physical Science and Technology and Department of Chemistry, University of Maryland, College Park, Maryland 20742

Raymond D. Mountain
Thermophysics Division, National Institute of Standards and Technology, Gaithersburg, Maryland 20899
(Received 3 August 1992)

The dynamics of the transition from supercooled liquid to glass is examined in terms of several probes: ergodic measures, self-diffusion coefficients, the Van Hove self-correlation functions, and the shear viscosity. Constant-pressure molecular-dynamics calculations at several temperatures are performed for a Lennard-Jones mixture and binary mixtures of soft spheres. The temperature dependence of the ergodicity diffusion parameters for both systems follow the Vogel-Fulcher law. On the other hand, the self-diffusion coefficients exhibit Arrhenius behavior for the soft-sphere system, but Vogel-Fulcher behavior for the Lennard-Jones system. These observations suggest that loss of effective ergodicity may be the universal feature of glass-forming substances. Various probes of the dynamics of the mixtures studied here suggest that the mechanism for mass transport dramatically changes from a simple diffusive process to one that involves activated transitions. The temperature at which this occurs is higher than the glass transition temperature T_g and lies in the range $1.1 < T/T_g < 1.3$. In this temperature range the effective ergodic times also increase very rapidly and suggest that the relaxation process is dominated by the presence of barriers in configuration space. We also show that the Stokes-Einstein relation between the shear viscosity and the self-diffusion coefficients starts to break down in the temperature range where the ergodic convergence times increase dramatically.

PACS number(s): 61.20.Ja, 61.43.Fs, 05.90.+m

I. INTRODUCTION

The mechanism for the dramatic increase in the viscosity as the temperature is lowered is not precisely known even for the simplest glass-forming substances. It has been difficult to identify the key characteristics of glassy materials that are largely independent of the intermolecular potential. The classification of glasses by Angell into "fragile" and "strong" has helped sharpen the question for theoretical approaches to glasses [1]. The models studied in this article are examples of "fragile" glasses, objects with two salient features. The first feature is a significant drop in the specific heat at constant pressure C_P as the temperature T approaches the glass transition temperature T_g. The second feature is that the temperature dependence of the viscosity, $\eta_s(T)$, clearly exhibits non-Arrhenius behavior at low enough temperatures and is often fitted by the celebrated Vogel-Fulcher functional form [2]. In a recent letter we argued that the "universal features" (ones that are independent of the precise intermolecular potential) of glass-forming substances can be understood in terms of loss in ergodicity as the degree of supercooling increases [3]. As a consequence the system is unable to overcome potential-energy barriers to diffusion on the time scale of observation. It is the purpose of this article to further develop and substantiate this idea. In addition, we provide arguments to show that the onset of a dramatic increase in the time scale needed for effective ergodicity to obtain is correlated with the change in the mechanism for single-particle diffusion.

One of the important recent discoveries about the strongly supercooled state of fluids characterized as fragile-glass formers is the presence of a dynamical transition which occurs at a temperature well above the laboratory glass transition temperature [4]. It is thought that this transition may be the physically significant, thermodynamic feature of the supercooled liquid, while the glass transition, which is known to depend on the way the state is prepared, is of less fundamental significance. This dynamical transition is thought to mark a change in the short-time translational motion of the molecules from small, continuous displacements to large, hopping steps which are separated by time intervals large compared with the duration of the step. In this picture, the transition is associated with the short-time localization of the particles rather than the freezing in of positions which occurs at the glass transition.

In contrast to the short-time localization of particles in a certain region of configuration space described above, the localization of the system in a potential-energy well for the system as a whole is the cause for certain thermodynamic properties, such as the decrease in the specific heat and changes in the nature of structural relaxation. In a microcanonical ensemble when the total energy E is greater than the characteristic barrier height E_B, the potential-energy-barrier picture is irrelevant and particle diffusion proceeded by the usual small displacement steps characteristic of Brownian motion. However, when the energy decreases to E_B the system encounters potential barriers of varying height. In this case it is useful to think in terms of "localization" of the system in a particular well for some time followed by an activated transi-

tion (probably involving a significant change in the positions of several particles) to a "neighboring" potential minimum.

This picture was proposed sometime ago by Goldstein [5], who argued that the slow structural relaxation process leading to the large viscosity in glassy states of matter is due to the existence of potential-energy barriers that are large compared to the thermal energy. Fluctuations, admittedly rare, must overcome these barriers for viscous flow to occur. Thus at low enough temperatures the system is essentially in a metastable well and is unable to make transitions to more favorable arrangements, at least on the time scale of observations. The duration of this localization condition is clearly dependent on the temperature. However, Goldstein estimated that it is meaningful to think about the process of localization in a specific well as soon as the relaxation time approaches about 10^{-9} s. In this spirit, one might argue that the system is basically localized in the metastable well for a time interval $t_B \approx \tau_0 \exp(E_B/k_B T)$, where τ_0 is a microscopic time $\approx 10^{-12}$ s, E_B is the typical barrier height, T is the temperature, and k_B is the Boltzmann constant. If the observation time scale is much less than t_B, which happens for $T \approx T_g$, then there is a breakdown of effective ergodicity.

Although this phenomenon of localization in a single potential-energy minimum does not readily lead to a theory of the liquid-to-glass transition, it offers useful insight into the topography of the potential-energy surface explored by glassy states. The basic notion of localization has already been used by Jónsson and Andersen [6] to rationalize the drop in heat capacity found in their computer simulations of binary mixtures of Lennard-Jones particles. In addition, recently van Megan, Underwood, and Pusey [7] have argued that the glass transition in "hard-sphere" colloidal glasses results in the localization of particles in an extremely long-lived metastable well. They have shown, using light-scattering experiments on polymethylmethacrylate particles dispersed in mixtures of decalin and carbon disulfide, that the onset of localization occurs over a narrow range of concentration of the particles.

In this study we attempt to distinguish between the particle localization in regions of configuration space that occurs near the dynamical transition temperature and the trapping of the system, at temperatures close to the glass transition temperature, in a long-lived, metastable free-energy minimum. It has long been appreciated that the loss of effective ergodicity is the general feature associated with the glass transition [8]. A system is said to be effectively ergodic if for a given time interval the system has equivalent time-averaged and ensemble-averaged properties [8,9]. As the glass transition is approached, the time interval necessary for effective ergodicity to be established increases rapidly and can become longer than the time available for observation. For the cases considered here the time available is the duration of a molecular-dynamics simulation. In this paper we use the energy-fluctuation metric introduced earlier [10,11] to determine the temperature dependence of the time interval needed to establish effective ergodicity of time averages for strongly supercooled Lennard-Jones mixtures and for the corresponding soft-sphere mixture. This is an extension of earlier work on a soft-sphere fluid [12,13] and shows that those results are not restricted to purely repulsive systems. We also examine the stress-fluctuation metric and compare the effective time interval estimates based on that metric with those based on the energy fluctuation metric.

The rest of the paper is organized as follows. The models examined and the definition of the energy-fluctuation metric are discussed in Sec. II. The ergodic convergence times, self-diffusion coefficients, and van Hove self-correlation functions are reported in Secs. III and IV. A portion of these results has been reported elsewhere [3,13]. Some concluding remarks based on these results are contained in Sec. V.

II. MODELS AND SIMULATION DETAILS

We have used the constant-pressure molecular-dynamics computer-simulation method with periodic boundary conditions [14] to examine the properties of a Lennard-Jones mixture and a mixture of soft spheres. The models are defined in terms of the interaction potential between a particle of type α located at position $\mathbf{r}_j$ and a particle of type β located at position $\mathbf{r}_k$. The Lennard-Jones interaction is

$$\phi_{\alpha\beta}(r_{jk}) = 4\varepsilon[(\sigma_{\alpha\beta}/r_{jk})^{12} - (\sigma_{\alpha\beta}/r_{jk})^{6}] , \tag{2.1}$$

where r_{jk} is the distance between sites $\mathbf{r}_j$ and $\mathbf{r}_k$. The soft-sphere interaction is

$$\phi_{\alpha\beta}(r_{jk}) = \varepsilon(\sigma_{\alpha\beta}/r_{jk})^{1/2} . \tag{2.2}$$

The systems consist of N_1 particles of type 1 with diameter $\sigma_{11} = 0.8\sigma_{22}$ and N_2 particles of type 2 with unit diameter $\sigma_{22} = 1$. The cross-interaction diameter $\sigma_{12} = 0.9\sigma_{22}$. The energy parameter ε is taken to have unit value. The mass of the type-2 particles is $m_2 = 1$ and the mass of the type 1 particles is taken to be $m_1 = 0.9m_2$. The unit of time is $\tau = [m_2\sigma_{22}^2/\varepsilon]^{1/2}$. The temperature is taken to be $\frac{2}{3}$ the mean kinetic energy per particle and is expressed in units of ε/k_B, where k_B is the Boltzmann constant. For the soft-sphere system the state of the system can be conveniently expressed in terms of an effective coupling constant $\Gamma = n^*(\sigma_{\text{eff}}/\sigma_{22})^3/(T^*)^{1/4}$. Here $n^* = N\sigma_{22}^3/V$, V is the volume of the system, $N = N_1 + N_2$, and σ_{eff} is the one-fluid van der Waals equivalent diameter [15,16].

For most of the simulations considered here we took $N_1 = 400$ and $N_2 = 100$ so that the composition variable $X = N_1/N = 0.8$. For the computation of the viscosity we took $N_1 = 81$ and $N_2 = 27$ so that $X = 0.75$. The smaller system size was used to keep the total computation time at a manageable level, as very long runs are necessary to obtain stable results for the viscosity.

The equations of motion were integrated using an iterated version of the Beeman algorithm [17] for the constant shape (cubic) cell using the Rahman-Parinello constant-pressure formulation of molecular dynamics [14] with a time step of 0.005τ. Two isobars $p = 5$ and

$p=0$ were examined for the Lennard-Jones mixture and one isobar $p=5$ was examined for the soft-sphere mixture. The glass transition temperature is $T_g=0.49$, for the Lennard-Jones $p=5$ isobar, $T_g=0.38$ for the $p=0$ isobar, and $T_g=0.08$ for the soft-sphere isobar. In terms of the coupling parameter Γ, the glass transition for the soft-sphere fluid occurs near $\Gamma=1.5$ [15]. The $p=0$ isobar reaches the liquid-vapor transition at $T\approx 1$, so the $p=5$ isobar was studied in order to extend the available temperature range.

III. DYNAMIC QUANTITIES

We have examined the dynamics of the systems by computing three types of quantities. The first involves examining single-particle motion in terms of the self-diffusion coefficients and the Van Hove self-correlation functions. The self-diffusion coefficients were determined using the Einstein relation for the mean-square displacement of the particles, which states that for long times, the self-diffusion coefficient D_α determines the slope of the mean-square displacement $R_\alpha^2(t)$ as a function of time ($\alpha=1,2$),

$$R_\alpha^2(t)=\frac{1}{N_\alpha}\sum_{j=1}^{N_\alpha}\langle[\mathbf{r}_{j\alpha}(t)-\mathbf{r}_{j\alpha}(0)]^2\rangle\rightarrow 6D_\alpha t \ . \tag{3.1}$$

The second quantities are the fluctuation metrics for the energy and stress, which provide estimates of effective ergodic convergence times. As discussed below, the Einstein relation for diffusion is closely related to the velocity-fluctuation metric. The G-fluctuation metric for a given property G is defined in terms of time averages of the quantity G_j associated with individual particles. We assume for the sake of notational simplicity that we have a one-component system. The extension of our results to multicomponent systems is straightforward [10,11]. An important notion for this discussion is that for a system in equilibrium, it is not possible to distinguish individual particles of a given type in terms of averaged properties associated with the individual particles. This is called statistical symmetry, a feature which is quite general for fluids [9,12].

The time average over the interval t of a single-particle property characterized by a phase function G_j is

$$g_j(t)=\frac{1}{t}\int_0^t ds\ G_j(s) \ . \tag{3.2}$$

Also, let $\bar{g}$ be the average of the $g_j(t)$'s, $\bar{g}=N^{-1}\sum_j g_t(t)$. A measure of the extent to which statistical symmetry is violated for a given averaging time t, namely, the G-fluctuation metric, is defined as

$$\Omega_G(t)=\frac{1}{N}\sum_{j=1}^{N}[g_j(t)-\bar{g}]^2 \ . \tag{3.3}$$

For an effectively ergodic system at long times $\Omega_G(t)$ obeys the scaling relation

$$\Omega_G(t)/\Omega_G(0)\rightarrow 1/D_G t \ , \tag{3.4}$$

where the G-metric coefficient D_G is a measure of the rate of ergodic convergence. This scaling relation can be derived by rewriting the definition of $\Omega_G(t)$ in terms of the time integral expression for $g_j(t)$ and invoking the equivalence of ensemble averages and time averages over a large enough sample for equilibrium states [10–12]. The result of this analysis is described in the Appendix.

In this paper we have considered several quantities for G, including the total energy of the ith particle,

$$G_i=E_i=p_i^2/2m+\sum_{j\ (\neq i)}\phi_{ij} \ , \tag{3.5}$$

and the off-diagonal element of the stress tensor,

$$G_i=S_i=\tfrac{1}{2}\sum_{k\ (\neq i)}\frac{x_{ik}y_{ik}}{r_{ik}^2}r_{ik}\frac{d\phi_{ik}}{dr_{ik}} \ , \tag{3.6}$$

where x_{ik} and y_{ik} are the x and y components of the vector $\mathbf{r}_{ik}$. We have also computed the metric with $G_i=V_{xi}$ the x component of the velocity of the ith particle. The energy- and stress-fluctuation metrics have been applied to fluids before [3,13]. The reason for considering the various physical candidates is to establish that the slowest relaxation process in supercooled liquids is associated with the difficulty in locating the bottleneck in configuration space which separates local energy minima. If the loss in ergodicity is the key issue in supercooled liquids near the glassy states, then it is necessary to demonstrate that other processes are in fact rapid compared to the time scales needed for effective ergodicity to be established (i.e., $D_E<D_S$).

We have argued in our earlier papers that the time behavior of $\Omega_E(t)$ allows us to infer if the system is localized in a free-energy well [9,11]. In particular, using a combination of $\Omega_E(t)$, which involves a single trajectory, and the energy metric, which compares two distinct trajectories, we showed that if the long-time value of $\Omega_E(t)\neq 0$, then this implies that the system is localized in a specific free-energy well. This should be distinguished from the localization of particles in specific regions of configuration space. The latter can in fact be examined by studying the time dependence of the mean-square displacement or the velocity-fluctuation metric $\Omega_V(t)$. A precise connection between the two can be made easily. The velocity metric is defined using Eq. (3.3) and the time-averaged values of the velocities of the individual particles.

Since $V_{xj}(t)=dX_j(t)/dt$ is the time rate of change of the x coordinate X_j of particle j, the time average of the x component of the velocity of particle j can also be written as

$$v_j(t)=\frac{X_j(t)-X_j(0)}{t} \tag{3.7}$$

and therefore, with the assumption that the total momentum of the system is zero, namely, that $\bar{v}=0$, it follows that

$$\Omega_V(t)=\frac{1}{N}\frac{\sum_{j=1}^{N}[X_j(t)-X_j(0)]^2}{t^2} \ . \tag{3.8}$$

This shows that the velocity fluctuation metric is related to the mean-square displacement by $t^2\Omega_V(t)=R^2(t)$. If the particles are free to diffuse, the numerator of Eq. (3.8) goes as $2D_{\rm self}t$ for long times and $\Omega_V(t)\rightarrow 1/D_V t$. However, if the particles are localized, the numerator will be bounded rather than increasing linearly with time and $\Omega_V(t)\rightarrow 1/t^2$. Thus $\Omega_V(t)$ contains the same information contained in $R^2(t)$, Eq. (3.1). It can be shown that $D_V=k_BT/D_{\rm self}m$, which implies that the time required for the velocities to equilibrate decreases as the degree of supercooling increases. This seemingly counterintuitive result is due to the increased efficiency in the exchange of momentum in the jammed state. When $D_{\rm self}$ vanishes, this relation ceases to be valid. Some properties of the fluctuation metrics are discussed further in the Appendix.

Also, this argument can be used to show that the force-fluctuation metric will always approach zero as $1/t^2$ for long times. To demonstrate this one need only repeat the argument associated with Eqs. (3.7) and (3.8) using the x component of the force on particle j, $F_{xj}(t)$, in place of $V_{xj}(t)$, $f_j(t)$, the time average of the x component of the force on particle j, in place of the $v_j(t)$, and $V_{xj}(t)$ in place of X_j. The result is

$$\Omega_F(t)=\frac{1}{N}\frac{\sum_{j=1}^{N}[V_{xj}(t)-V_{xj}(0)]^2}{t^2} . \tag{3.9}$$

Because the velocity moments are always localized in velocity space, the force-fluctuation metric will go as $1/t^2$ for all states. The time required to reach this long-time-limiting behavior is determined by the relatively short time required to sample velocity space. Consequently, for systems interacting via simple pair potentials, the force-fluctuation metric proves to be uninteresting.

The hallmark of glasses is the dramatic increase in the shear viscosity as the temperature is lowered. A direct estimate of η_s from computer simulation is difficult due to the nature of the averaging required and due to the long relaxation times involved [18]. We have calculated η_s as a function of T with $p=5$ for the Lennard-Jones mixture with $X=0.75$ and $N=108$. We used the Einstein relation [19], which states for long times that

$$\eta_s=\frac{n}{2k_BT}\frac{d}{dt}\left\langle\left[\sum_{j=1}^{N}\int_0^t ds\,\sigma_j^{\alpha\beta}(s)\right]^2\right\rangle , \tag{3.10}$$

where σ_j^{xy} is the off-diagonal part of the stress tensor. This transport coefficient, which involves many-particle correlations instead of only single-particle correlations, is the third type of quantity calculated.

IV. RESULTS

A. Ergodicity coefficients D_E and D_S

The simulations were performed at several temperatures at constant pressure for a Lennard-Jones mixture and for a two-component soft-sphere mixture. The fluctuation metrics for the off-diagonal stress and for the energy were calculated and the corresponding coefficient D_G ($G=E$ or S) were obtained from the long-time behavior of $\Omega_G(t)$. The temperature dependence of D_E and D_S is displayed in Fig. 1. The main part of Fig. 1 is for the Lennard-Jones mixture at a pressure $p=5$. Inset (a) is for the $p=0$ Lennard-Jones case and inset (b) is for the soft-sphere mixture.

There are two principal comments about these results that are worth making: (i) At all temperatures $D_S>D_E$, which implies that the relaxation of local stresses takes place more rapidly than does the exploration of available configuration space, the process probed by the energy-fluctuation metric [11]. For the Lennard-Jones mixture, D_S is considerably larger than D_E. The difference is less pronounced for the soft-sphere mixture. This suggests that the slowest process is associated with the ability of the system to overcome barriers in configuration space. (ii) It is also clear that the Arrhenius form cannot fit the temperature dependence of D_E and D_S over the entire temperature range. We examined power-law representations of these coefficients of the form $D=a(T-T_g)^x$. The Vogel-Fulcher representation provides a more uniform set of parameters than does the power law, so we do not consider that representation further. We have previously shown [3] that our data for D_E can be adequately fitted by the Vogel-Fulcher form and we find this to be the case for D_S as well, i.e.,

$$D_G=A_G\exp[-B_G/(T-T_0)] , \tag{4.1}$$

where the subscript G can be either E or S. In Fig. 1 the symbols indicate the computed values and the solid line is a Vogel-Fulcher representation of the computed values. The Vogel-Fulcher parameters were determined by first finding a value for T_0 such that a semilog plot of D vs $1/(T-T_0)$ was linear. Next, the slope of that plot pro-

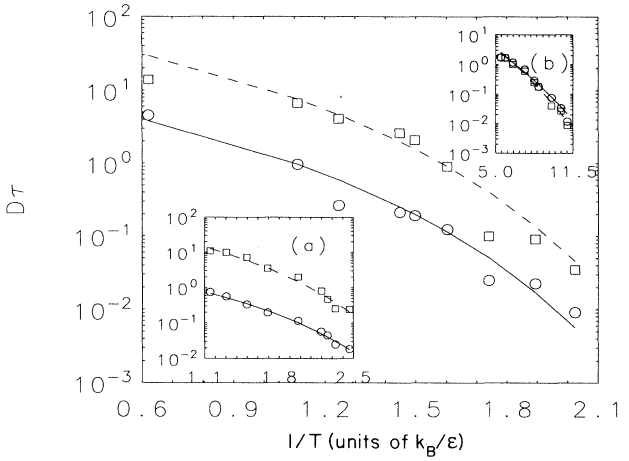

FIG. 1. The fluctuation metric coefficients D_E (circles) and D_S (squares) as a function of $1/T$ are displayed in the main figure for the Lennard-Jones mixture with $p=5$. The results for the $p=0$ mixture are displayed in insert (a) and those for the soft-sphere mixture are displayed in insert (b). The lines are the Vogel-Fulcher fits to the computed values using the parameters from Table II. Similar behavior is found for the type-2 particles, which is not shown here.

TABLE I. The Vogel-Fulcher parameters for the fluctuation metric coefficients D_E and D_S are listed for the three isobars examined.

Isobar	$A_E\tau$	$B_E(\varepsilon/k_B)$	$A_S\tau$	$B_S(\varepsilon/k_B)$	$T_0(\varepsilon/k_B)$
Lennard-Jones, $p=5$	12.37	1.550	95.0	1.54	0.29
Lennard-Jones, $p=0$	3.22	1.017	73.0	1.15	0.21
Soft-sphere, $p=5$	50.4	0.469	86.3	0.54	0.03

vides a value for B and the value of A was obtained from the intercept of that plot. *A common value of T_0 was used for D_E and D_S.* The values of the adjustable parameters A, B, and T_0 are listed in Table I. These values of T_0 can be used to compute the "fragility factor," which is defined to be $F=T_g/(T_g-T_0)$ [1]. The value of F for the soft-sphere mixture is 1.6, whereas it is 2.5 for the Lennard-Jones mixture. The difference between these values of F helps us rationalize the distinct temperature dependences of the self-diffusion coefficients in these systems, which is noted below. Because of the large cooling rates employed in computer simulations it is easy to see that F for computer glasses would be smaller than laboratory values.

It is interesting to estimate the approximate time scale required for effective ergodic convergence to be obtained in these systems. Figure 2 exhibits the temperature dependence of the effective ergodic convergence time τ_E obtained from the energy-fluctuation metric using the empirical relation

$$\tau_E = 100/D_E \ , \tag{4.2}$$

which was introduced earlier by us [10,12]. This empirical relation seems to give an adequate estimate for τ_E for several properties, including the time for convergence of dipole moment fluctuations in water [20]. Equation (4.2) is based on the interpretation that D_E is proportional to the rate of exploration of the available configuration space. If τ_E exceeds the observation time $\tau_{\rm obs}$ then it is clear that effective ergodicity is broken. This implies that energetically acceptable configurations belonging to distinct potential-energy minima for strongly supercooled liquids are separated by bottlenecks in configuration space such that the system is unable to locate these regions in the time $\tau_{\rm obs}$. Under these conditions one can say that the system is localized in a particular energy (or free-energy) minimum and structural relaxation can only take place by an activated mechanism. Figure 2 shows the dramatic increase in τ_E in a relatively narrow temperature range. The potential-energy-barrier picture discussed above starts to become relevant as soon as $\tau_E \approx 1$ ns [5], which would correspond to $T \approx 1.5 T_g$. Thus long before the glass transition is approached we expect the nature of transport to change. This is further corroborated by a detailed study of the Van Hove self-correlation function, which is discussed below.

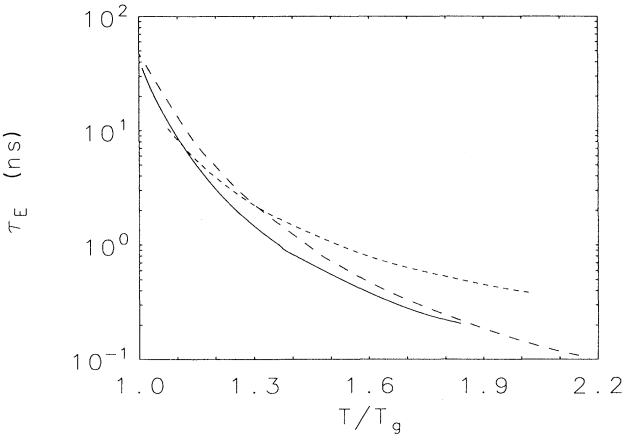

FIG. 2. Ergodic convergence times [Eq. (3.1)] as functions of T/T_g for the $p=5$ Lennard-Jones mixture (solid line), for the $p=0$ Lennard-Jones mixture (short-dashed line), and for soft-sphere mixture (long-dashed line). These times are based on argonlike values for the units such that $\tau = 2\times 10^{-12}$ s.

B. Self-diffusion coefficients

The temperature dependence of the self-diffusion coefficients is shown in Fig. 3. Again, the results can be represented in the Vogel-Fulcher form. The fitting parameters are shown in Table II. Note that T_0 for the soft-sphere fluid is not distinguishable from zero for the self-diffusion coefficient, while it is clearly greater than

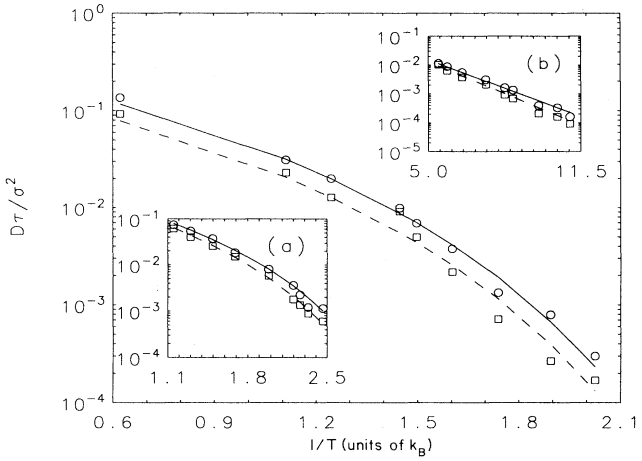

FIG. 3. The self-diffusion coefficients for type-1 particles as a function of $1/T$ are displayed in the main figure for the Lennard-Jones mixture with $p=5$. The results for the $p=0$ mixture are displayed in inset (a), and those for the soft-sphere mixture are displayed in inset (b). The lines are the Vogel-Fulcher fits to the computed values using the parameters from Table II. Similar behavior is found for the type-2 particles, which is not shown here.

TABLE II. The Vogel-Flucher parameters for the self-diffusion coefficients D_1 and D_2 are listed for the three isobars.

Isobar	$A_1(\sigma^2/\tau)$	$B_1(\varepsilon/k_B)$	$A_2(\sigma^2/\tau)$	$B_2(\varepsilon/k_B)$	$T_0(\varepsilon/k_B)$
Lennard-Jones, $p=5$	0.36	1.48	0.25	1.52	0.29
Lennard-Jones, $p=0$	0.51	1.22	0.49	1.34	0.21
Soft-sphere, $p=5$	0.48	0.69	0.62	0.77	0.00

zero for the energy metric and stress metric coefficients. The qualitative difference in the temperature dependence of the self-diffusion coefficients of the soft-sphere and Lennard-Jones mixtures suggests that the dynamics in the supercooled states for these systems is quite different. Since the interaction between the soft-sphere particles is purely repulsive, single-particle diffusion through interstices or holes can take place without significant rearrangement of neighboring particles if these holes can accommodate the particle. For solids it is known that vacancy diffusion follows the Arrhenius law and this analogy may indeed be useful for the soft-sphere system [21]. On the other hand, because of the tendency of the Lennard-Jones particles to form icosahedral structures at low temperatures [6], large length-scale fluctuations could occur if a single particle in the cluster undergoes significant displacement. This is a qualitative picture that naturally accounts for the difference in the effective barrier heights for diffusion, which in the Lennard-Jones system is twice that for the soft-sphere mixture (see Table II). Although this physical picture is relatively useful in explaining the faster decrease of D_1 and D_2 for the Lennard-Jones mixtures than for the soft-sphere mixtures, it does not lead to an explanation for the nonzero values of T_0 for the Lennard-Jones mixture. However, the effectively Arrhenius behavior of the self-diffusion coefficients for the soft-spheres but not for the energy-fluctuation metric emphasizes that the universal characteristics of glass-forming substances are displayed only in quantities that manifestly monitor the ergodicty of the system.

C. Van Hove functions and particle localization

The ergodicity parameter D_E gives only the overall time required for the system to explore the allowed regions of configuration space in a coarse-grained sense. In order to gain additional insight into the nature of the particle dynamics we have also computed the van Hove self-correlation function $G_\alpha(r,t)$, which provides a detailed description of the motion of the individual particles of species α. This function has been computed before for soft-sphere mixtures [22], for a Lennard-Jones mixture using constant-temperature molecular dynamics [23], for a molten salt [24], and for methanol [25]. The van Hove self-correlation function for particles of type α is

$$G_\alpha(r,t)=\frac{1}{N_\alpha}\left\langle \sum_{i=1}^{N_\alpha}\delta(|\mathbf{r}_i(t)-\mathbf{r}_i(0)|-r)\right\rangle , \tag{4.3}$$

where $\mathbf{r}_i(t)$ is the position of particle i of species α at time t. At high temperatures it is expected to closely match the form derived from the diffusion equation solution. The diffusion model states that $G_\alpha(r,t)$ is the solution to

$$\frac{\partial G_\alpha(r,t)}{\partial t}=D_\alpha\nabla^2 G_\alpha(r,t) \tag{4.4}$$

with the initial condition

$$G_\alpha(r,0)=\delta(r) . \tag{4.5}$$

That solution is [26]

$$G_\alpha(r,t)=(1/4\pi D_\alpha t)^{3/2}\exp(-r^2/4D_\alpha t) \tag{4.6}$$

and is normalized so that

$$\int_0^\infty 4\pi r^2 G_\alpha(r,t)dr=1 . \tag{4.7}$$

Thus persistent deviations from the diffusive behavior would be indicative of a change in the mechanism of single-particle dynamics from small step diffusive motion to a difference mechanism.

In the following discussion, the calculated values of $P_\alpha(r,t)=4\pi r^2 G_\alpha(r,t)$, the distribution of particles of type α which have moved a distance r in a time t, are compared with the form of Eq. (4.6). The $p=5$ states of the

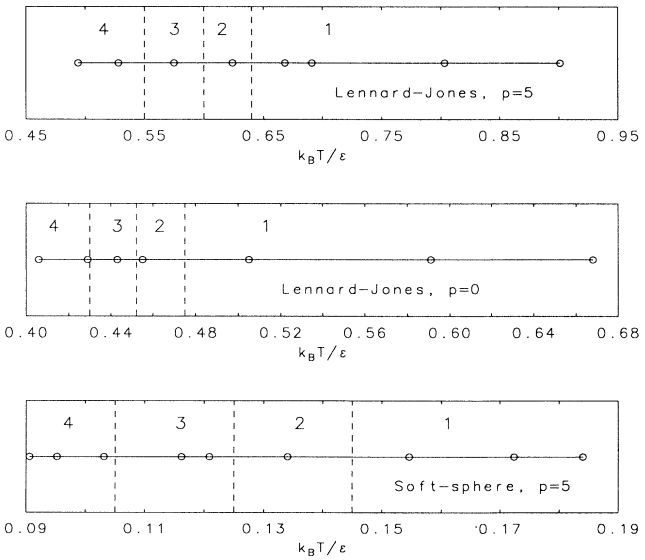

FIG. 4. The temperature domains for the four types of time dependence exhibited by the Van Hove self-correlation functions are shown. The circles indicate the temperatures where the functions were constructed and the vertical dashed lines roughly indicate the boundaries of these domains.

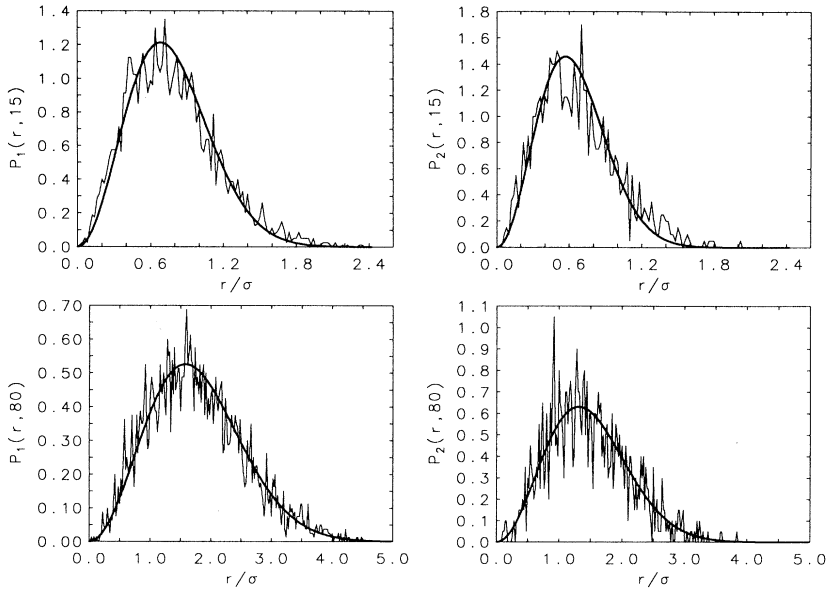

FIG. 5. Typical time and space behavior of $P(r,t)$ for the temperature domain 1. The plots on the left-hand side are for type-1 particles and those on the right-hand side are for type-2 particles. The jagged line represents the computed values with $\Delta r = 0.01\sigma_{22}$, and the bold solid line represents the diffusion solution, Eq. (4.6), evaluated with the calculated value of the self-diffusion coefficient D_α.

Lennard-Jones mixture are used as illustrations. Similar behavior of the distributions is also found for the $p=0$ states of the Lennard-Jones mixture and for the $p=5$ states of the soft-sphere mixture. There are four temperature regions to be noted, which are identified by numerals in Fig. 4. It should be emphasized that the boundary between these regions is not meant to be sharp. In Figs. 5–8, the computed $P_\alpha(r,t)$ is represented by a solid, jagged line and the diffusion form, Eq. (4.6) evaluated using the computed value for the self-diffusion coefficient, is represented by a smooth, bold, solid line.

At high temperatures, which we indicate as region 1, the calculated distributions and the diffusion solution coincide for times $t > 5\tau$, the smallest time interval examined. This is illustrated in Fig. 5, where these quantities are displayed for both species at a temperature of $T = 0.666 \approx 1.4 T_g$. The upper set of plots is at $t = 15\tau$ and the lower set of plots is at $t = 80\tau$.

As the temperature is lowered the first type of deviation of the computed distributions occurs at early times and for displacements of less than one particle diameter. This is shown in the upper part of Fig. 6 for the

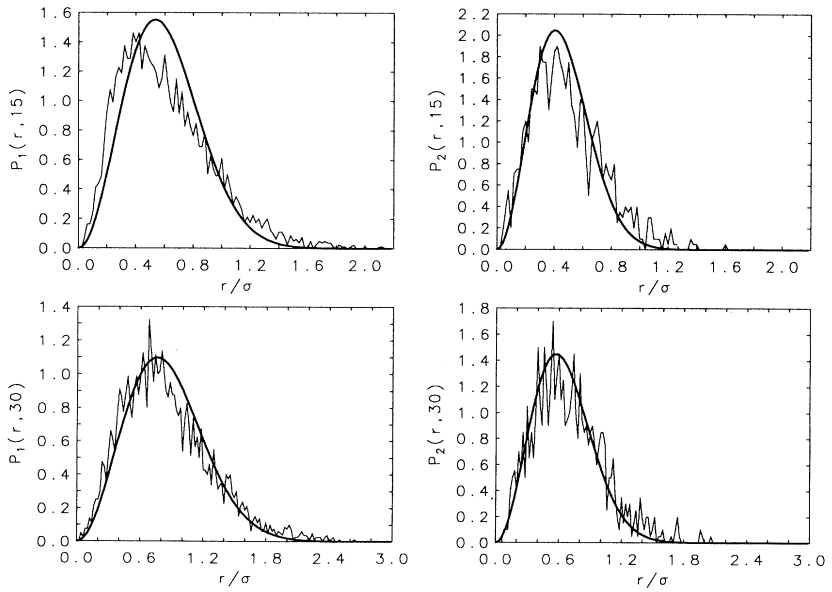

FIG. 6. Typical time and space behavior of $P(r,t)$ for the temperature domain 2; same layout as in Fig. 5.

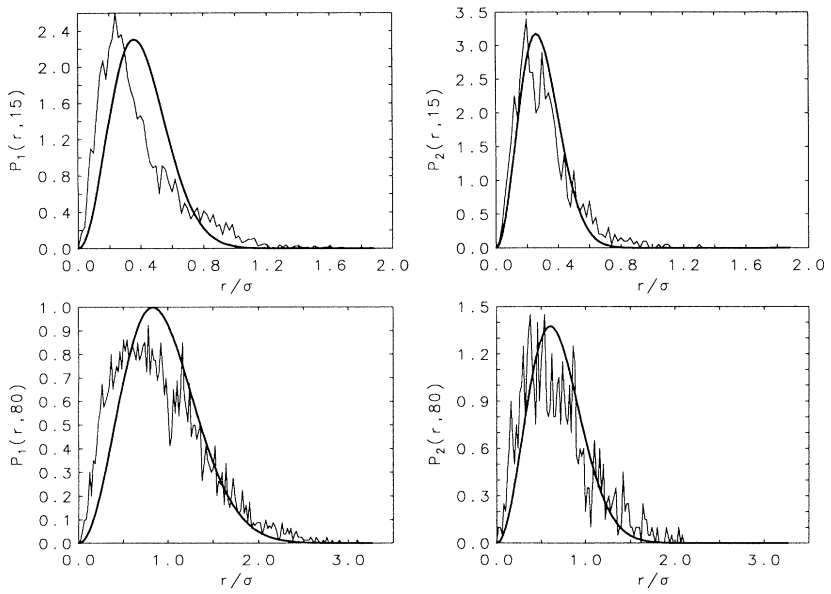

FIG. 7. Typical time and space behavior of $P(r,t)$ for the temperature domain 3; same layout as in Fig. 5.

$T=0.621\approx 1.3T_g$ state at a time $t=15\tau$. The peak of the diffusive solution is at a larger distance than the computed peak. This disagreement disappears at longer times, as shown in the lower part of Fig. 6 at the time $t=30\tau$. This we call region 2. The distinction between regions 1 and 2 is arbitrary as it depends only on the time interval needed for the computed values of $P_\alpha(r,t)$ to match the diffusion solution.

Further lowering of the temperature leads to a more significant difference between the diffusion solution and the computed distributions in that the number of particles which have moved a distance greater than $\frac{1}{2}\sigma$ is significantly greater than the diffusive prediction. This is shown in Fig. 7 for the $T=0.575\approx 1.2T_g$ state. The upper set is for $t=15\tau$ and the lower set is for $t=80\tau$. This we call region 3, where it is evident that particle transport does not happen by a diffusive process. In this regime it is reasonable to suggest that single-particle dynamics proceeds by some sort of cooperative "hopping" process. Notice that even at $T=0.575\approx 1.2T_g$ there is an apparent change in the dynamic mechanism for particle motion. This conclusion is consistent with several experimental observations [27] and suggests that this temperature may correspond to the rounded dynamic transition predicted by mode-coupling theory [28].

There is another feature that emerges as the temperature is lowered further into region 4. A significant fraction of the particles do not move very far from their ini-

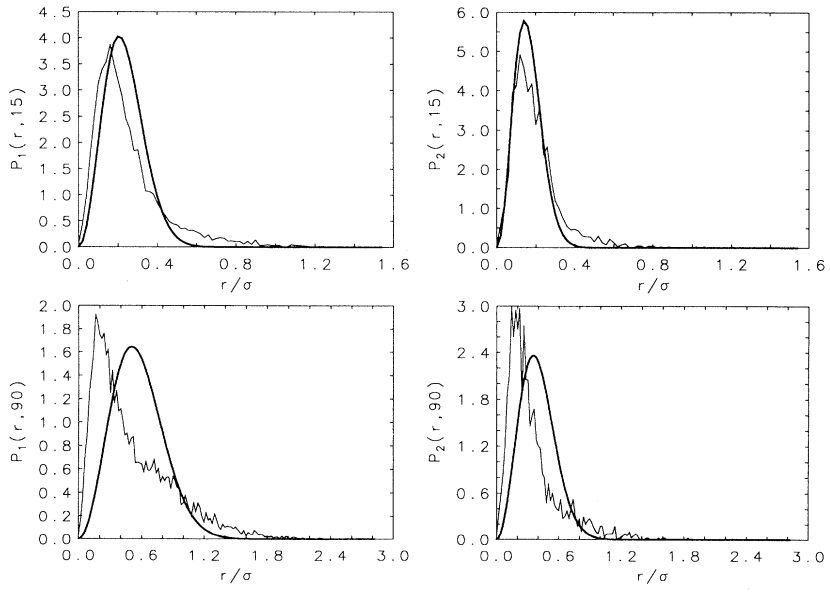

FIG. 8. Typical time and space behavior of $P(r,t)$ for the temperature domain 4; same layout as in Fig. 5.

tial position during the observed time interval of 100τ. This is shown in Fig. 8 for the $T=0.536\approx 1.1T_g$ state. The upper set is for $t=15\tau$ and the lower set is for $t=90\tau$. In this region both hopping and localization of particles is present. Since the process of hopping necessarily involves an activation barrier we expect that for times less than the typical hopping time the particles would be essentially localized. This localization is different from the localization of the system in a particular energy minimum. In the former case the positions of particles are restricted to a certain region in configuration space. In the latter case the set of all of the coordinates of the particles would map onto a specific minimum. It is interesting that the change in mechanism occurs over a narrow temperature range $\sim 0.1T_g$. These observations are consistent with the dynamic light-scattering experiments on colloidal glasses [7] in which the onset of particle localization over a narrow density range was demonstrated.

When the temperature is lowered still further the mobility of the particles is further reduced, and eventually no "diffusion" is observable during the 100τ observation period. At that point, the glassy state has formed.

D. Viscosity and the Stokes-Einstein relation

The shear viscosity η_s was evaluated using Eq. (3.10). The calculated values of the shear viscosity for the Lennard-Jones mixture are displayed in Fig. 9 as a function of $1/T$. The non-Arrhenius behavior is evident. The solid line is a Volger-Fulcher fit with $T_0=0.29$ and $B=1.5$, values close to those appropriate to the metrics and the self-diffusion coefficients. At the lowest temperature where a reliable value of the viscosity could be determined, there is an indication that the Volger-Fulcher representation is inadequate. The inset shows a power-law representation of the viscosity,

$$\eta_s = a/(T-T_g)^x , \tag{4.8}$$

with $a=1.0$ and $x=2$. This power-law form provides a better fit for the viscosity than it did for the metric and self-diffusion coefficients. The uncertainty in the computed value of the viscosity for $T<0.55$ is large enough that the deviation from power-law behavior at low temperature cannot be excluded. The power law obtained for η_s, valid for $T>0.55$, is in good accord with the predictions of mode-coupling theory [28,29].

The viscosity and self-diffusion results can be used to check the validity of the Stokes-Einstein relation, $D_\alpha = k_B T/2\pi\eta_s d_\alpha$, where d_α is the Stokes diameter for particles of type $\alpha=1,2$ and is nearly independent of temperature for liquids [30]. The quantity $\eta_s D_\alpha/T$ is plotted in Fig. 10. For temperatures greater than about 0.7, it is effectively independent of temperature but at lower temperatures it increases rapidly. This indicates a change in the diffusion and/or viscosity mechanisms. For the strongly supercooled states, the viscosity increases more rapidly than the self-diffusion coefficient decreases, behavior that leads to a *decreasing* Stokes diameter. Among other things, the breakdown of the Stokes-Einstein relation implies that the Stokes diameter is not to be identified with a correlation length which increases as the glass transition is approached. The origin of this temperature variation is not known and warrants further study. It may be another indication of the "dynamical transition" discussed above. it is interesting to note that the temperature where the Stokes-Einstein relation fails is roughly $1.3T_g$, a value which is consistent with the estimates for change in the mechanisms for structural relaxation based on the study of D_E and the dynamics of the Van Hove function. Similar behavior of the self-diffusion coefficients and the viscosity have been found in a soft-sphere mixture [31] and in data for fragile-glass formers [32].

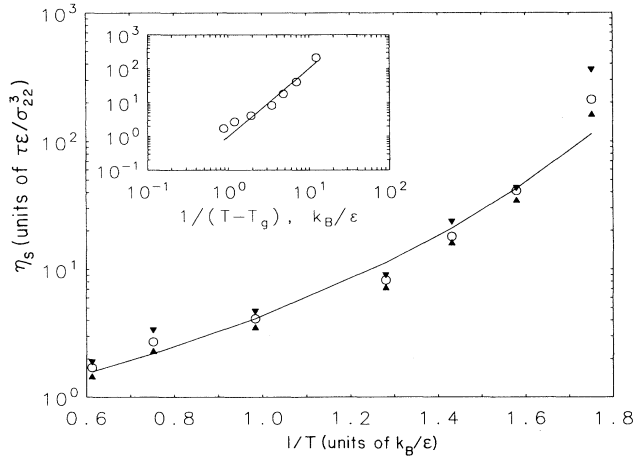

FIG. 9. The temperature dependence of η_s for the $p=5$, $X=0.75$ Lennard-Jones mixture. The solid curve in the main plot shows Vogel-Fulcher representation. The triangles indicate the uncertainties in the calculated values of the viscosity. The inset shows the power-law fit.

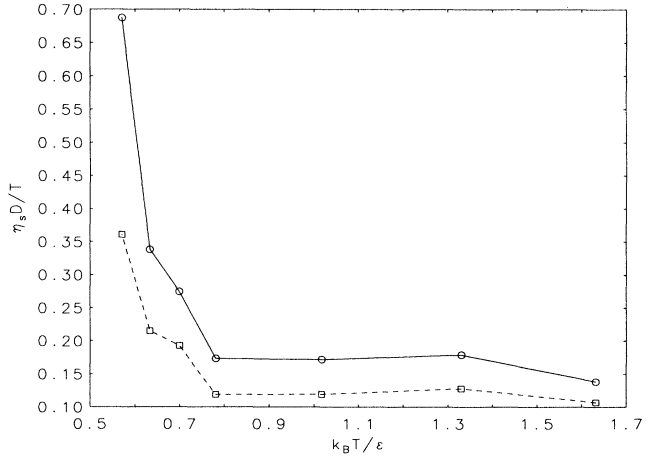

FIG. 10. The temperature dependence of $\eta_s D/T$ for the $p=5$ Lennard-Jones mixture with $X=0.75$.

V. CONCLUSIONS

In this paper we have presented results of extensive constant-pressure simulations for a Lennard-Jones mixture and for binary soft-sphere alloys. We have computed several quantities pertaining to transport in supercooled liquids, namely, the self-diffusion coefficients, the shear viscosity, the Van Hove self-correlation function, and the ergodic convergence parameters D_E and D_S. We conclude this paper with the following remarks.

The time variation of quantities such as the energy-fluctuation metric and the energy metric [9] is a useful probe of localization of the system in a free-energy well. In particular, if the long-time behavior of $\Omega_E(t) \neq 0$, then one can conclude that the system is effectively trapped in a particular free-energy minimum for times on the order of D_E^{-1}. On the other hand, localization of particles in a region of configuration space is better examined by studying the Van Hove self-correlation function. This distinction, brought out by this study, is important because even if the system is localized in a given free-energy minimum, there are examples, such as superionic conductors [33], where single-particle diffusive motion exists.

The temperature dependence of the self-diffusion coefficients for the soft-sphere mixtures and the Lennard-Jones system show distinctly different behavior. For the soft-sphere system, D_1 and D_2 obey a simple Arrhenius law, whereas for the Lennard-Jones mixtures these coefficients show clear deviations from a simple activated expression and are better represented by a Vogel-Fulcher law. On the other hand, the ergodic convergence coefficients for both types of mixtures exhibit non-Arrhenius behavior. The potential-energy-barrier picture of Goldstein appeals to general, universal notions about the energy landscape. Thus any quantity that gives an indication of the dynamics of exploration in this complex energy profile should exhibit universal behavior as long as the statistical characteristics of this profile are similar. The parameter D_E^{-1} sets the time scale for adequate sampling of the configurations belonging to distinct minima. The similarity in the behavior of D_E for both systems suggests that the key mechanisms for slow structural relaxation is a dramatic rise in the ergodicity time scale. This feature leads us to conclude that the loss of ergodicity, brought about by the presence of bottlenecks with a distribution of barrier heights in the complex potential-energy surface, is the fundamental controlling feature for relaxation in glassy systems. This argument is further buttressed by noting that the time scale for other physical quantities is shorter than that for the energy.

The results presented here also dramatically show the failure of the Stokes-Einstein relation in highly supercooled liquids near the glass transition. This has been observed before by analyzing NMR data on organic and inorganic glass formers [32]. It has been argued that the temperature range where the Stokes-Einstein relation starts to fail is indicative of a change in the diffusion mechanism, an interpretation consistent with ours. This temperature range is typically well above the glass transition temperature. The analysis of the various dynamical quantities lead us to suggest that this crossover region is roughly $1.1T_g - 1.3T_g$. The nature of the failure of the Stokes-Einstein relation excludes it, or equivalent statements, from identifying the Stokes diameter with a growing correlation length in glass-forming substances. We have come to similar conclusions using the ergodicity time τ_E in the expression

$$\xi \approx (k_B T \tau_E / \eta_s)^{1/3} \tag{5.1}$$

for an effective correlation length. Instead, it may be necessary to explicitly introduce quantities which are spatially distributed [34].

It is heartening to note that in all the fits of the various quantities the values of T_0 are basically the same and only depend on the pressure. This suggests a robustness about the existence of an ideal glass transition even though kinetic considerations prevent simulations from actually probing the dynamics near T_0. By combining our results with the notion of entropically driven transitions it is possible in principle to identify a diverging correlation length ξ near $T \approx T_0$. Since the cooling rate are extraordinarily high in computer simulations, the quantity $t = (T - T_0)/T_0$ is quite large at the kinetic glass transition temperature. For our cases the value of $t_g = (T_g - T_0)/T_0$ ranges from 0.7 to 2.0, which implies that the value of ξ is at best of the order of 2–3 molecular diameters. Thus at present it is not possible to probe the divergence of ξ ($\sim t^{-\nu}$, $\nu = 2/d$) [34,35] using computer simulations. This explains the failure to find a diverging correlation length in computer simulations of glasses [36].

ACKNOWLEDGMENTS

This work was supported in part by grants from the National Science Foundation and the Camille and Henry Dreyfuss Foundation.

APPENDIX

The general form of the fluctuation metric for a quantity G is

$$\Omega_G(t)/\Omega_G(0) = \frac{2}{t}[\mathcal{J}_0(t) - (1/t)\mathcal{J}_1(t)] , \tag{A1}$$

where

$$\mathcal{J}_0(t) = \int_0^t ds\, C_G(s) \tag{A2}$$

and

$$\mathcal{J}_1(t) = \int_0^t ds\, s C_G(s) . \tag{A3}$$

The time correlation of the individual particle fluctuations in G, $C_G(t)$, is normalized to unity at $t = 0$.

There are three types of long-time behavior for the metrics of condensed-matter systems which are in stationary, but not necessarily thermodynamic equilibrium, states. The first type of long-time behavior, which we label I, applies to systems which are ergodic. For case I,

$$\Omega_G(t)/\Omega_G(0) \rightarrow \frac{1}{D_G t} , \tag{A4}$$

where D_G is proportional to the reciprocal of the time integral of the single-particle fluctuation correlation function.

The second type of behavior, which we label II, applies to systems for which the time integral of the single-particle fluctuation correlation function does not reach a limiting value for long times. This occurs if the time correlation function does not decay to zero, but instead reaches a finite, long-time value. In this case, $\mathcal{J}_0(t)$ is proportional to t for long times and $\Omega_G(t)/\Omega_G(0)$ approaches a constant, nonzero value for long times. This is what happens with the energy-fluctuation metric in a glassy state.

The third type of behavior, which we label III, occurs for variables for which $\mathcal{J}_0(t)$ is zero for long times. (This is the case called an "oscillatory variable" by Rahman [37].) Then $\Omega_G(t)/\Omega_G(0)$ is proportional to $1/t^2$ for long times with the constant of proportionality being $-2\mathcal{J}_1(t)$, which approaches a positive constant for long times.

The types of time dependence exhibited by metrics as a function of supercooling depends on the type of variable being considered. The energy metric exhibits type-I behavior for fluid states and type-II for glassy states. The velocity metric on the other hand exhibits type-I behavior for fluid states but type-III behavior for glassy states. The force fluctuation metric exhibits *only* type-III behavior.

It is worth emphasizing that the velocity and energy are inherently different type of variables, and thus the time dependence of the corresponding metrics is will be different. Consider what happens as the liquid is supercooled. For the energy-fluctuation metric, the magnitude of D_E decreases rapidly, indicating that the time needed to sample configuration space is growing rapidly. On the other hand, the velocity-metric coefficient, $D_V \propto 1/D_{\text{self}}$, *increases* rapidly with decreasing temperature, indicating that the time required to sample momentum space decreases as the mobility of the particles decreases. This relation ceases to hold when D_{self} is identically zero, i.e., when the velocity is an oscillatory variable.

[1] C. A. Angell, J. Phys. Chem. Solds **49**, 863 (1988).

[2] G. W. Scherer [J. Am. Ceram. Soc. **75**, 1060 (1992)] has written an interesting commentary on the history of this representation.

[3] R. D. Mountain and D. Thirumalai, Phys. Rev. A **45**, R3380 (1992).

[4] J. Ullo and S. Yip, Phys. Rev. A **39**, 5877 (1989).

[5] M. Goldstein, J. Chem. Phys. **51**, 3328 (1969).

[6] H. Jónsson and H. C. Andersen, Phys. Rev. Lett. **60**, 2295 (1988).

[7] W. van Megen, S. M. Underwood, and P. N. Pussey, Phys. Rev. Lett. **67**, 1586 (1991).

[8] R. G. Palmer, Adv. Phys. **31**, 669 (1982).

[9] D. Thirumalai, R. D. Mountain, and T. D. Kirkpartick, Phys. Rev. A **39**, 3563 (1989).

[10] R. D. Mountain and D. Thirumalai, J. Phys. Chem. **93**, 6975 (1989).

[11] D. Thirumalai and R. D. Mountain, Phys. Rev. A **42**, 4574 (1990).

[12] R. D. Mountain and D. Thirumalai, Int. J. Mod. Phys. C **1**, 77 (1990).

[13] R. D. Mountain and D. Thirmulaai, in *Slow Dynamics in Condensed Matter,* edited by K. Kawasaki, M. Tokuyama, and T. Kawakatsu, AIP Conf. Proc. No. 256 (AIP, New York, 1992), p. 165.

[14] M. Parrinello and A. Rahman, J. Appl. Phys. **52**, 7182 (1981). The original molecular-dynamics constant pressure method is due to H. C. Anderson, J. Chem. Phys. **72**, 2384 (1980).

[15] G. Pastore, B. Bernu, J. P. Hansen, and Y. Hiwartai, Phys. Rev. A **36**, 4891 (1987).

[16] R. D. Mountain and D. Thirumalai, Phys. Rev. A **36**, 3300 (1987).

[17] D. Beeman, J. Comput. Phys. **20**, 130 (1975).

[18] J. J. Erpenbeck, Phys. Rev. A **38**, 6255 (1988).

[19] C. Hoheisel and R. V. Vogelsang, Comput. Phys. Rep. **8**, 4 (1988).

[20] R. D. Mountain and D. Thirumalai, Comput. Phys. Commun. **62**, 352 (1991).

[21] S. Mazur, J. Chem. Phys. **93**, 3542 (1990).

[22] J. N. Roux, J. L. Barrat, and J.-P. Hansen, J. Phys. Condens. Matter **1**, 7171 (1989).

[23] G. Wahnström, Phys. Rev. A **44**, 3752 (1991).

[24] G. F. Signorini, J.-L. Barrat, and M. L. Klein, J. Chem. Phys. **92**, 1294 (1990).

[25] P. Sindzingre and M. L. Klein, J. Phys. Chem. **96**, 4681 (1992).

[26] J. P. Hansen and I. R. McDonald, *Theory of Simple Liquids* (Academic, New York, 1986), p. 257.

[27] F. Mezei, J. Non-Cryst. Solids **131**, 317 (1991). This article contains references to earlier work. It also provides a critical assessment of what the experiments do and do not say about the mode-coupling predictions.

[28] W. Götze and L. Sjögren, Rep. Prog. Phys. **55**, 241 (1992).

[29] E. Leutheusser, Phys. Rev. A **29**, 2765 (1984); U. Bengtszehius, W. Götze, and A. Sjölander, J. Phys. C **17**, 5915 (1984); T. R. Kirkpatrick, Phys. Rev. A **31**, 939 (1985).

[30] J. P. Hansen and I. R. McDonald, *Theory of Simple Liquids* (Ref. [26]), p. 210.

[31] J.-L. Barrat, J.-N. Roux, and J.-P. Hansen, Chem. Phys. **149**, 197 (1990).

[32] E. Rössler, J. Non-Cryst. Solids **131**, 242 (1991).

[33] See, e.g., *The Physics of Superionic Conductors and Electrode Materials,* Vol. 92 of NATO Advanced Study Institute, Series B: Physics, edited by J. P. Perram (Plenum, New York, 1980).

[34] E. W. Fischer, E. Donth, and W. Steffen, Phys. Rev. Lett. **68**, 2344 (1992).

[35] T. R. Kirkpartick, D. Thirumalai, and P. G. Wolynes, Phys. Rev. A **40**, 1045 (1989).

[36] R. M. Ernst, S. R. Nagel, and G. S. Grest, Phys. Rev. B **43**, 8070 (1991); R. O. Rosenberg, D. Thirumalai, and R. D. Mountain, J. Phys. Condens. Matter **1**, 2109 (1989); C. Dasgupta, A. V. Indrani, S. Ramaswamy, and M. K. Phani, Europhys. Lett. **15**, 307 (1991).

[37] A. Rahman, in *Statistical Mechanics, New Concepts, New Problems, New Applications,* edited by S. A. Rice, K. F. Freed, and J. C. Light (University of Chicago Press, Chicago, 1971), p. 177.